4527.
3. Nam, K. C.; Kim, J. M.; Kim, D. S. *Bull. Korean Chem. Soc.* **1995,** *16,* 186.
4. Park, Y. J.; Shin, J. M.; Nam, K. C.; Kim, J. M.; Kook, S.-K. *Bull. Korean Chem. Soc.* **1996,** *17,* 643.
5. Gutsche, C. D.; Lin, L.-G. *Tetrahedron* **1985,** *41,* 1633.
6. Iqbal, M.; Mangiafico, T.; Gutsche, C. D. *Tetrahedron* **1987,** *43,* 4917.
7. Nam, K. C.; Kim, J. M.; Kook, S. K.; Lee, S. J. *Bull. Korean Chem. Soc.* **1996,** *17,* 499.
8. Jaime, C.; Mandoza, J. D.; Parados, P.; Nieto, P. M.; Sanchez, C. *J. Org. Chem.* **1991,** *56,* 3372.
9. Iwamoto, K.; Yanaki, A.; Arimura, T.; Matsuda, T.; Shinkai, S. *Chem. Letters* **1990,** 1901.
10. Zetta, L.; Wollf, A.; Vogt, W.; Platt, K.-L.; Bohner, V. *Tetrahedron* **1991,** *47,* 1911.
11. Iwamoto, K.; Shimizu, J. D.; Araki, K.; Shinkai, S. *J. Am. Chem. Soc.* **1993,** *115,* 3997.

# Motional Properties in the Structure of GlcNAc( β 1,3)Gal( β )OMe Studied by NMR Spectroscopy and Molecular Modeling

**Gyuchang Shim, Sangwon Lee, and Yangmee Kim***

*Department of Chemistry, Konkuk University, Seoul 143-701, Korea*
*Received February 5, 1997*

Conformational flexibilities of the GlcNAc( β 1,3)Gal( β )OMe are investigated through NMR spectroscopy and molecular modeling. Adiabatic energy map generated with a dielectric constant of 50 contains three local minima. All of the molecular dynamics simulations on three local minimum energy structures show fluctuations between two low energy structures, N2 at φ=80° and ψ=60° and N3 at φ=60° and ψ= −40°. We have presented adequate evidences to state that GlcNAc( β 1,3)Gal( β )OMe exists in two conformationally discrete forms. Two state model of N2 and N3 conformers with a population ratio of 40 : 60 is used to calculate the effective cross relaxation rate and reproduces the experimental NOEs very well. Molecular dynamics simulation in conjunction with two state model proves successfully the dynamic equilibrium existed in GlcNAc( β 1,3)Gal( β )OMe and can be considered as a powerful method to analyze the motional properties in the structure of carbohydrate. This observation also cautions against the indiscriminate use of a rigid model to analyze NMR data.

## Introduction

Cell membranes must interact with their external environment as a part of important biological processes such as cell recognition, intercellular adhesion, and regulation of growth and de fence against invading organisms. The interactions are usually achieved by binding of a protein to a carbohydrate receptor anchored to the cell membrane as a part of glycoprotein or glycolipid. These carbohydrates have the biological functions which control the several intracellular reactions as recognition signals.[1,2] Accordingly, knowledge of structural details of such protein-carbohydrate interactions is fundamental to understand the interaction of cell and its environment.[3,4]

N-acetylglucosamine residue occurs in glycoproteins, glycolipids, and proteoglycans with a variety of structures. One of the linkages commonly found in all three classes of glycoconjugates is GlcNAc( β 1,3)Gal. Repeating units of this disaccharide are present in certain mucins, membrane glycoproteins, and polyglycosylceramides where they are associated with the Ii-antigenic structures and serve as precursors of the ABH, Lewis, and $P_1$ blood group antigens.[5-7] Specially, lectins such as Wheat Germ Agglutinin (WGA) and Limulus polyphemus agglutinin (LPA) recognize the carbohydrates which contain GlcNAc as a terminal sugar residue in the membrane. Study of interactions between the WGA and various carbohydrate containing GlcNAc is our on going project.

According to the our previous NMR study it is found that free lactose and free melibiose exist with a variety of conformational flexibility and there are considerable confirmational changes of melibiose induced by binding to ricin.[8,9] It shows tendency of protein binding to restrict conformational freedom about glycosidic bond. In order to understand the structural details of such protein-carbohydrate interactions it is nececesary to study the structural changes of oligosaccharide as a recognition signal. Here, structure of β-D-GlcNAc-[1-3]- β-D-Gal-1-OMe (GlcNAc( β 1,3)Gal( β )OMe) which can be a receptor for proteins having GlcNAc specificity is studied using nuclear magnetic resonance spectroscopy, adiabatic energy map, and molecular dynamics simulation.[10-12]

NMR is the best method to provide structural data in solution where motional variations are less restricted than in crystals. The nuclear Overhauser effects used to evaluate interproton distance constraints are also susceptible to large variations because of the unusual way that motional averaging can affects the measured parameters. It is important to consider the possibility that the assumption of a static structure, implicit in most structure determination protocols,

is inappropriate.[14,15] In the present study, we have carried out the confirmational analysis of GlcNAc( β 1,3)Gal( β )OMe with complete internal flexibility by NMR spectroscopy in conjunction with molecular modeling. We propose two state model to represent the motional averaging existed in GlcNAc( β 1,3)Gal( β )OMe.

## Experimental

**Nomenclature.** Figure 1 shows the naming scheme of the GlcNAc( β 1,3)Gal( β )OMe molecule constructed by N-acetyl glucosamine (GlcNAc) and galactose (Gal) rings through the ( β 1,3) glycosidic bond. Flexibilities around the glycosidic linkages are described by the following two torsion angles: φ and ψ are defined as H1'-C1'-O3-C3 and C1'-O3-C3-H3, respectively, as shown in Figure 1. χ is defined as O5-C5-C6-O6. Three possible orientations relative to C5 and C6 are designated as GT, GG, and TG and depicted in Figure 2. θ is defined as C1'-C2'-N2'-C7' which determines the orientation of N-acetyl group.

**NMR experiments.** GlcNAc( β 1,3)Gal( β )OMe was purchased from Sigma. The NMR samples were lyophilized repeatedly from 99.9% $D_2O$, and dissolved in 100% $D_2O$ under a nitrogen atmosphere and 10 mM sample is made in 0.4 mL.

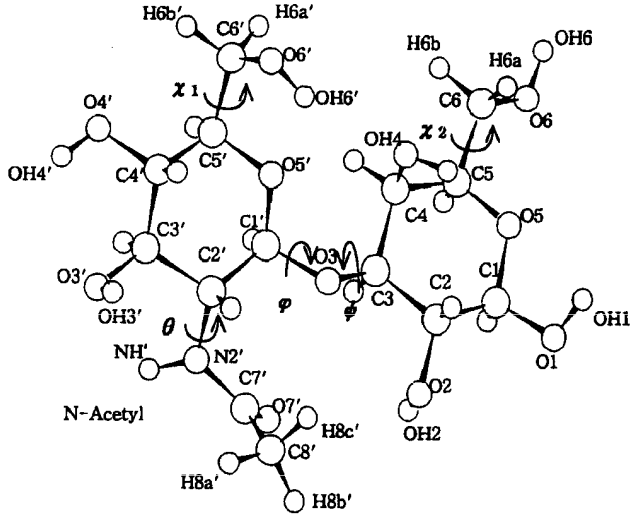


**Figure 1.** Low energy structure of GlcNAc( β 1,3)Gal( β )OMe. The dihedral angles, φ, ψ, $\chi_1$, $\chi_2$, and θ are defined as H1'-C1'-O3-C3, C1'-O3-C3-H3, O5'-C5'-C6'-O6', O5-C5-C6-O6, and C1'-C2'-N2'-C7', respectively.

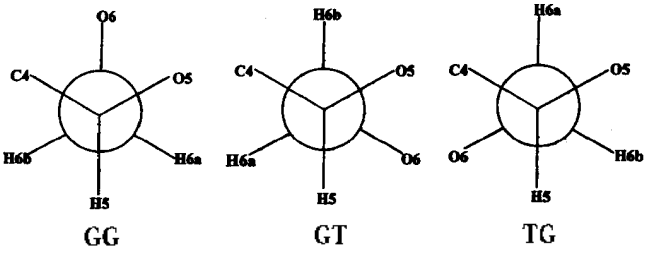


**Figure 2.** Definition of the exocyclic conformation of a six membered sugar ring. GG, GT, TG. G represents gauche (60°), and T represents trans (180°). The first letter means the orientation of O5-C5-C6-O6 and the second letter means the orientation of C4-C5-C6-O6.

NMR experiments were performed at 30 °C on a Bruker AMX 500 MHz spectrometer at Inter-University Instrument Institute at Seoul National University. All the data were processed off-line using FELIX software on SGI workstation in Department of Chemistry at Konkuk University.[15] For spectral assignments a double quantum filtered COSY spectrum was obtained using time proportional phase incrementation (TPPI) with spectral width of 1754.386 Hz, 4096 $t_2$ point, and 512 $t_1$ point. Due to the large degree of spectral overlap, we collected a TOCSY spectrum with a mixing time of 80 msec and a $^1H$-$^{13}C$ heteronuclear multiple quantum coherence (HMQC) spectrum to aid the spectral assignments.[16,17] As well, a high resolution 1D spectrum (64 K) was acquired to determine coupling constant accurately. 2D $^1H$-$^1H$ phase sensitive NOESY and ROESY experiment was performed with mixing times of 600 and 800 msec.[18,19]

Exocyclic orientation of the terminal sugar is very important in fitting to the binding site of the protein. In the previous study we derived the scalar coupling equations to evaluate the dihedral constraints about C5-C6 using Haasnoot' s modified Karplus equations as follows.[10,20] Here, χ is an exocyclic dihedral angle explained in Figure 1.

$$^3J_{5,6} = 13.22\cos^2\chi - 0.99\cos\chi - 2.61 - 0.984\{\cos^2(\chi - 7.96)\} - 3.198\{\cos^2(-\chi - 25.87)\} - 3.198\{\cos^2(\chi - 25.87)\} \quad (1\text{-}1)$$

$$J_{5,6} = 13.22\cos^2\chi + 0.99\cos\chi + 2.61 - 0.984\{\cos^2(\chi + 7.96)\} - 6.396\{\cos^2(-\chi + 25.87)\} \quad (1\text{-}2)$$

**Adiabatic energy map.** All calculations were performed with CHARMM (Chemistry at HARvard Macromolecular Mechanics). The potential function of CHARMM is as follows.[15,21]

$$V(q) = k_b(r - r_0)^2 + k_\theta(\theta - \theta_0)^2 + k_{ub}(s - s_0)^2 + k'_{ub}(s, s_0)^2 + ki[1 + \cos(n\phi_i - \delta_i)] + \sum k_i(\omega_i - \omega_{i0})^2 + \sum\left(\frac{A_{ij}}{r_{ij}^{12}} - \frac{B_{ij}}{r_{ij}^{6}}\right) + \sum\frac{q_i q_j}{4\pi\varepsilon_0 r_{ij}} \quad (2)$$

Eq. 2 contains the terms such as bond energy, angle energy, dihedral energy, Urey-Bradley 1-3 interaction energy, improper energy, electrostatic energy, and van der Waals energy. Hydrogen bond energy term is not handled separately, but treated as nonbonding interactions in the CHARMM potential. Parameters used in this study is available through QUANTA.[15]

Energy surface for molecules as complicated as GlcNAc ( β 1,3)Gal( β )OMe usually has many minima. In order to solve the local minima problem, we performed minimization for a set of systematically selected initial geometries and generated adiabatic energy map.[10-12] Conformational energy of GlcNAc( β 1,3)Gal( β )OMe depends not only on the torsion angle of the glycosidic bond but also on the intraring hydrogen bonding patterns of hydroxyl groups, and the orientation of exocyclic hydroxymethyl group and N-acetyl group. Therefore, these confirmational respects are considered in preparing the energy map based mainly on constrained values of φ and ψ.

Due to the strong electrostatic interactions, hydroxyl groups in a monosaccharide ring form hydrogen bonds

between each other with all the OH vectors pointing the same direction around the ring in vacuum. Following the atomic numbering of carbon atoms increasing clockwise, we designate the clockwise pattern of intraring hydrogen bonding as "C". The reverse-clockwise pattern of intraring hydrogen bonding is designated as "R".[12]

The adiabatic potential energy map is generated as follows. First, flexibilities in GlcNAc and Gal monomeric rings are studied with paying special attentions to the orientation of hydroxyl groups in the monomeric ring. Minimization is performed with 30° increments of exocyclic hydroxymethyl group and this minimized structures are utilized in generating initial geometries of GlcNAc( β 1,3)Gal( β )OMe. In the second step, the minimized conformations of two rings are patched to generate the starting structure of GlcNAc( β 1,3)Gal( β )OMe at each grid point in ( φ, ψ) space. There are four possible combinations of the disaccharide ring conformation in regard to the intraring hydrogen bonding arrangements: RR, RC, CR, and CC. The orientations of N-acetyl group and the exocyclic hydroxymethyl groups are also considered for each dimer conformation. Each combined conformation at a grid point of φ and ψ (20° in spacing) is minimized with 200 steps of steepest descent (SD) minimizer and subsequently with adopted basis Newton-Raphson (ABNR) minimizer with the constraints on the glycosidic bond until the root-mean-square (rms) gradient becomes less than 0.001 Kcal/mol. The energy contour is finally refried around each local minimum. All of the energy map in this paper are relaxed maps generated with constrained values of φ and ψ but optimized in all other degrees of freedom.

It is of primary interest to investigate confirmational details of GlcNAc( β 1,3)Gal( β )OMe in an aqueous medium. In the potential energy functions in equation 2 the dielectric medium effect can be incorporated into the electrostatic energy term through the dielectric constant. Without explicit solvent molecules, the medium effect of dielectric screening can be effectively mimicked by increasing the dielectric constant. According to the study on lactose, we found that the electrostatic energy is a slow varying function of the dielectric constant above 10. Dielectric constant of 50 suppresses effectively the overemphasized electrostatic interaction and reproduces the experimental data of lactose very well. Therefore, we calculated adiabatic energy maps with a dielectric constant of 1 (in vacuum) and 50.

## Results and Discussion

The proton resonance assignment in free GlcNAc( β 1,3) Gal( β )OMe was proceeded on the basis of DQF-COSY and HMQC spectrum shown in Figure 3 and 4. Since there are large degree of symmetry of sugar rings, a number of proton resonances were found to be degenerated and made the measurement of the NOE and the coupling constant difficult. Heteronuclear correlated experiments such as HMQC and HMBC was used to complete assignment. In Figure 4 assignment of the carbon spectrum is shown. Table 1 lists chemical shift and coupling constant data for GlcNAc( β 1,3) Gal( β )OMe. $^3J_{3,4}$, $^3J_{4,5}$, $^3J_{4,5}$, $^3J_{5,6a}$, and $^3J_{5,6b}$ values are consistent with both rings residing in $^4C_1$ chair conformations. $^3J_{1,2}$ and $^3J_{1,2}$ are consistent with both rings having β -link-

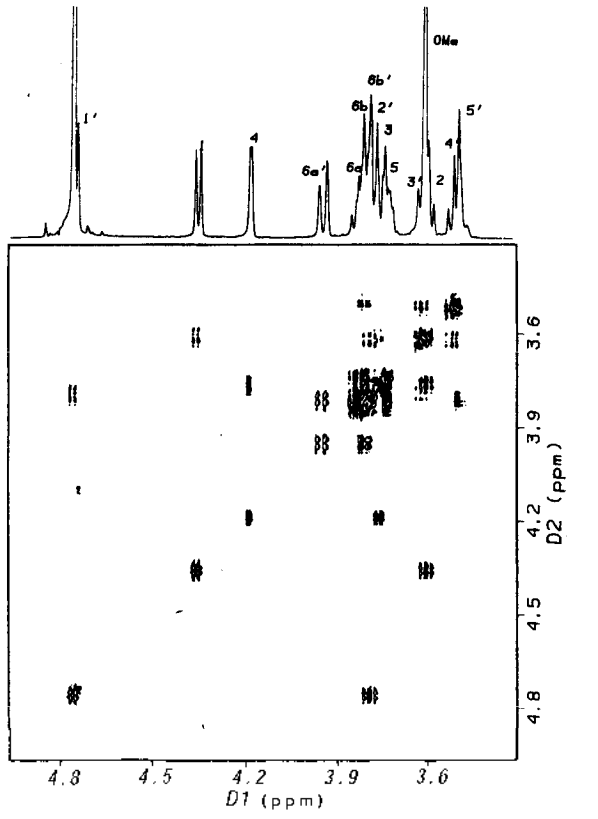


**Figure 3.** 500 MHz $^1$H NMR spectrum of 10 mM GlcNAc( β 1,3) Gal( β )OMe at 303 K. On the top 1D $^1$H NMR spectrum of GlcNAc( β 1,3)Gal( β )OMe is shown and DQF-COSY spectrum is shown below.

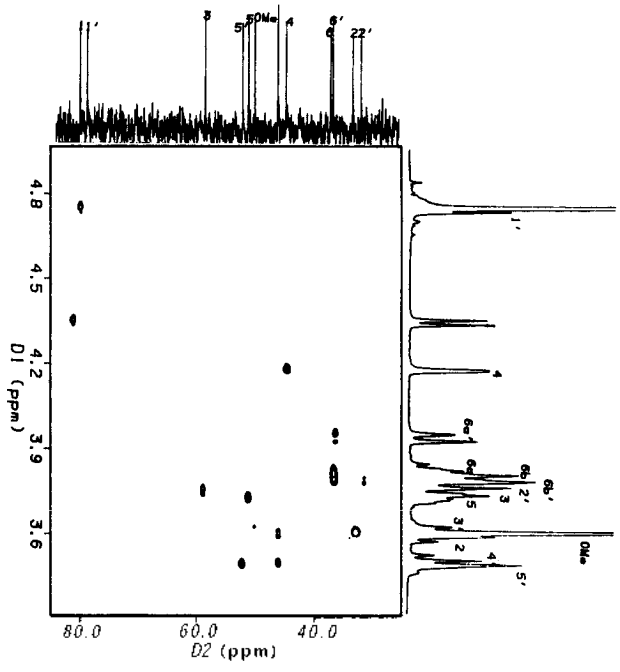


**Figure 4.** Phase sensitive, $^{13}$C-decoupled, $^1$H detected multiple-quantum correlation (HMQC) spectrum of 10 mM GlcNAc( β 1,3) Gal( β )OMe at 303 K and 500 MHz.

**Table 1.** Chemical shifts and scalar couplings of GlcNAc( β 1,3) Gal( β )OMe

| Proton | σ (ppm)[a] | Proton pair | J (Hz)[b] |
|---|---|---|---|
| H1' | 4.74 | H1'-H2' | 7.8 |
| H2' | 3.80 | H2'-H3' | 10.8 |
| H3' | 3.61 | H3'-H4' | 7.9 |
| H4' | 3.52 | H4'-H5' | |
| H5' | 3.49 | H5'-H6a' | 3.3 |
| H6a' | 3.95 | H5'-H6b' | 4.7 |
| H6b' | 3.81 | H6a'-H6b' | 12.5 |
| H1 | 4.36 | H1-H2 | 7.8 |
| H2 | 3.61 | H2-H3 | 9.4 |
| H3 | 3.76 | H3-H4 | 3.2 |
| H4 | 4.19 | H4-H5 | 3.1 |
| H5 | 3.73 | H5-H6a | |
| H6a | 3.87 | H5-H6b | |
| H6b | 3.83 | H6a-H6b | |
| OMe | 3.61 | | |

[a]Chemical shift of the HDO peak was set at 4.75 ppm. [b]Digital Resolution is 0.054 Hz/point (1D) and 0.43 Hz/point (2D).

ages. On the top of the Figure 3 assignment of the 1D spectrum is shown. As shown in this spectrum chemical shift of the most of the ring protons are crowded between 3.5 and 4. 2 ppm except the anomeric protons. H5-H6a, H5-H6b, and H6a-H6b coupling constants in the first ring are not measured because of the spectral overlap. However, H5'-H6a', H5'-H6b', and H6a'-H6b' coupling constants are measured and they provide information about the exocyclic orientation of terminal GlcNAc ring. An-ride proton in the N-acetyl group and all of the hydroxyl protons are exchanged with deuterium within 1 minutes and it implies that this amide proton does not form any intramolecular hydrogen bond in aqueous solution.

Distance information derived from NOE data as well as rotamer distribution calculated from coupling constants should lead to definition of the solution structure of free GlcNAc( β 1,3)Gal( β )OMe. As reported in the other papers[4,7] the observed values of $^3J_{5,6a}$ and $^3J_{5,6b}$ are sensitive to the rotamer distributions about the C5-C6 bond. The coupling constants measured from NMR experiment are $^3J_{5,6}$=3.3 Hz, $^3J_{5,6b}$=4.7 Hz. $^3J_{5,6a'}$ calculated theoretically using equation 1 is 2.8 Hz for GG, 3.1 Hz for GT, and 10.7 Hz for TG orientation. $^3J_{5,6b'}$ calculated theoretically using equation 1 is 0.9 Hz for GG, 10.7 Hz for GT, and 5.0 Hz for TG orientation. Population ratio between GG, GT, and TG orientations for the terminal GlcNAc ring which shows the best fit to the experimental coupling constants is calculated as 50 : 40 : 10.

Figure 5 shows the ROESY spectrum with a mixing time of 800 msec. The distance information obtained from NOESY and ROESY experiments with mixing times of 600 msec and 800 msec are listed in Table 2. Particular interest would be imposed on the protons around the glycosidic linkage. The interresidue NOEs such as H1'-H2, H1'-H3, and H 1'-H4 are very important to determine the conformation of GlcNAc( β 1,3)Gal( β )OMe. For the calibration, distance between H1'-H5' was set to 2.44 Å and this distance is the value in charmm-minimized structures. Since there are limited number of NOEs, theoretical study can provide more information about the structure and dynamics of GlcNAc( β 1,

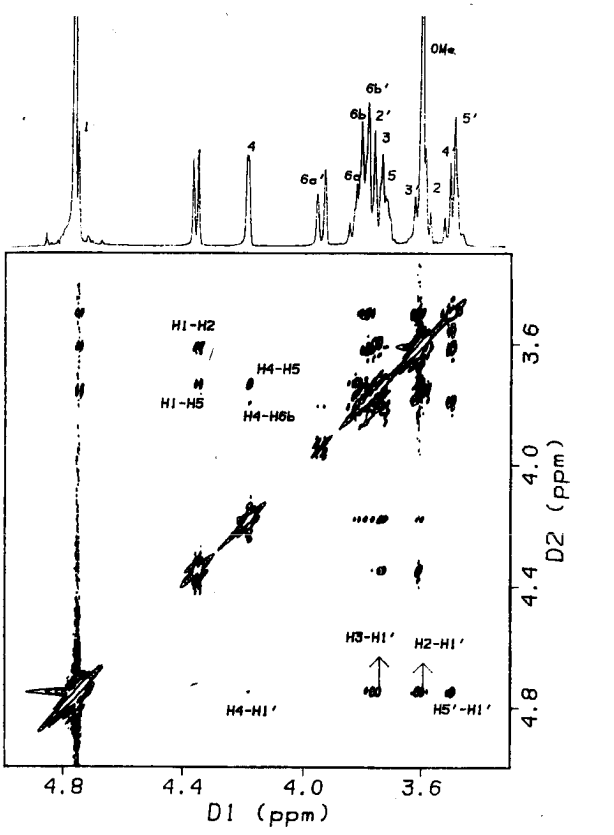


**Figure 5.** 500 MHz $^1$H ROESY spectrum of 10 mM GlcNAc( β 1,3)Gal( β )OMe in D$_2$O at 303 K. Mixing time of 800 msec was used.

**Table 2.** Distances obtained from NOE of GlcNAc( β 1,3)Gal( β )

| Proton pair | Distance (Å) |
|---|---|
| H2-H1' | 3.2 |
| H3-H1' | 2.5 |
| H4-H1' | 4.0 |
| H2'-H1' | 2.5 |
| H3'-H1' | 2.8 |
| H5'-H1' | 2.4 |
| H3-H4 | 2.5 |
| H5-H4 | 2.6 |
| H6a-H4 | 3.5 |
| H6b-H4 | 3.0 |
| H5'-H6b' | 2.5 |

The H5'-H1' distance was set to 2.44 Å

3)Gal( β )OMe.

Figure 6 shows the adiabatic energy map of GlcNAc( β 1, 3)Gal( β )OMe in vacuum. It shows three local minima corresponding to relatively low energy conformations of GlcNAc( β 1,3)Gal( β )OMe. They are designated as N1, N2, and N3, respectively. Table 3 lists a set of the selected torsion angles and distances of the low energy conformers of GlcNAc( β 1,3)Gal( β )OMe located on the energy map generated in vacuum. N1 at φ=20° and ψ=40° is the lowest energy conformation in vacuum. The values for the glycosidic torsion angles φ and ψ are almost totally responsible for the overall shape of the disaccharide since they define the relative position of the fairly inflexible sugar ring. N1 is

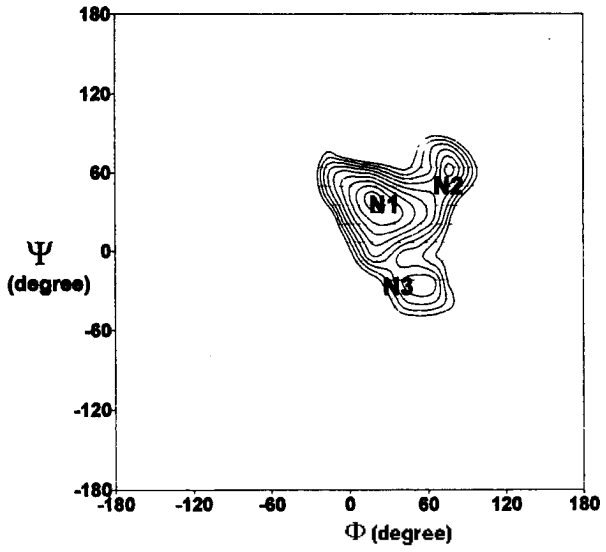


**Figure 6.** Adiabatic energy map of GlcNAc( β 1,3)Gal( β )OMe generated in vacuum. Contours are in 0.5 kcal mol intervals from 0.5 to 5.0 kcal mol above the energy minimum. Three low energy structures are designated as N1, N2 and N3.

**Table 3.** Conformational features and relative energy of the minimum energy conformations found on the vacuum energy map

| | φ | ψ | $\chi_L$ | $\chi_D$ | θ | H2-H1' | H3-H1' | H4-H1' | HBOND | Relative |
|---|---|---|---|---|---|---|---|---|---|---|
| | (degree) | | | | | | (Å) | | | (kcal/mol) |
| N1 | 20 | 40 | 19 | 35 | 155 | 3.5 | 2.4 | 4.3 | O7'-OH3' O2-NH' | 0.0 |
| N2 | 80 | 60 | 32 | 34 | 156 | 2.7 | 3.3 | 4.7 | O7'-OH3' O2-OH6' | 1.48 |
| N3 | 60 | -20 | 0 | 35 | 167 | 4.2 | 2.3 | 3.8 | O7'-OH3' | 2.39 |

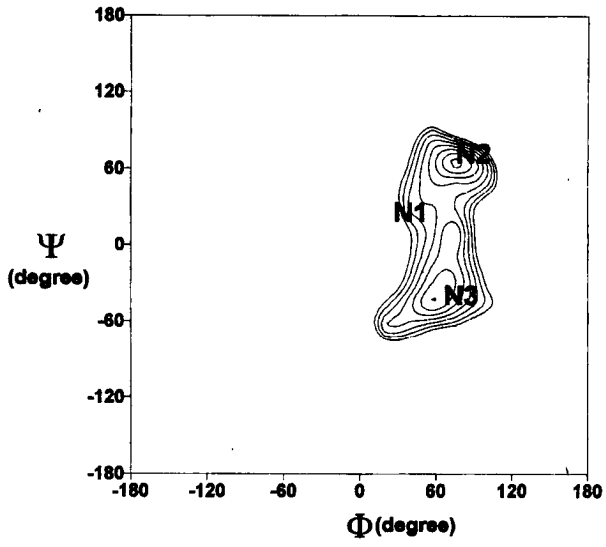


**Figure 7.** Adiabatic energy map of GlcNAc( β 1,3)Gal( β )OMe generated with a dielectric constant of 50. Contours are in 0.3 kcal/mol intervals from 0.3 to 2.1 kcal mol above the energy minimum. Three low energy structures are designated as N1, N2 and N3.

**Table 4.** Conformational features and relative energy of the minimum energy conformations found on energy map generated with a dielectric constant of 50

| | φ | ψ | $\chi_L$ | $\chi_D$ | θ | H2-H1' | H3-H1' | H4-H1' | Relative |
|---|---|---|---|---|---|---|---|---|---|
| | (degree) | | | | | (Å) | | | (kcal/mol) |
| N1 | 40 | 40 | -50 | 70 | 162 | 3.1 | 2.1 | 4.4 | 1.715 |
| N2 | 80 | 60 | -48 | 70 | 162 | 2.7 | 3.3 | 4.7 | 0.0 |
| N3 | 60 | -40 | -48 | 71 | 89 | 4.3 | 2.4 | 3.5 | 0.399 |

characterized as GTGT-RR where GT denotes the exocyclic orientation of the first and the terminal sugar rings, and RR denotes the intraring hydrogen bonding patterns. N1 has two intramolecular hydrogen bonds from the N-acetyl group. Those are O7'-OH3' with the distance of 1.8 Å and O2-NH' with the distance of 2.0 Å.

The other local minima N2 and N3 are all characterized as GTGT-RR, too. N2 at φ=80° and ψ=60° has two hydrogen bonds of O7'-OH3' with a distance of 1.8 Å and O2-OH6' with a distance of 2.1 Å. N3 at φ=60°and ψ= -20°has also hydrogen bond O7'-OH3' with a distance of 1.8 Å. The intramolecular hydrogen bonds are the dominant structural factors in constructing the lowest energy conformation of carbohydrate in vacuum. Distances of H1'-H2, H1'-H3, and H1'-H4 are the major interest because they show the close NOE contacts listed in Table 2. N1 reproduces the structural constraints determined by the NMR experiments such as H1'-H2, H1'-H3, and H1'-H4 distances better than the other low energy conformations in the vacuum map. While amide proton of N-acetyl group in N1 conformation forms a stable intramolecular hydrogen bond, deuterium exchange experiment shows that the exchange rate of this amide proton is very fast and proves that in aqueous solution amide proton in N-acetyl group does not form any intramolecular hydrogen bond. No solvent effect is incorporated into the vacuum map calculation and structural features can be different from the NMR experimental data.

In order to consider the solvent effect in energy map calculation, the adiabatic energy map of GlcNAc( β 1,3)Gal( β )OMe was calculated with a dielectric constant of 50. According to our previous studies on disaccharides, it is appropriate to replace explicit water molecules working as the solvent by the dielectric constant larger than 10.[10,11] The increased dielectric constant in the potential energy function suppresses overemphasized electrostatic energy terms including hydrogen bond strength, and removes intramolecular strain imposed by nonbonded interactions, which is what solvent molecules do in effect. Energy map is generated with the dielectric constant of 50 and it is shown in Figure 7. The overall feature of the energy map calculated with a dielectric constant of 50 is similar to that calculated in vacuum. Adiabatic energy map calculated with a dielectric constant of 50 shows three local minima corresponding to relatively low-energy conformation of GlcNAc( β 1,3)Gal( β )OMe. Table 4 lists a set of the selected torsion angles and distances of the low energy conformers of GlcNAc( β 1,3)Gal( β )OMe located on the energy map calculated with a dielectric constant of 50. While the global minimum N1 in the vacuum energy map becomes one of the local minimum on the dielectric energy map, the energy of N2 and N3 be-

comes lower than the energy of N1 in the dielectric map. The energy of N2 and N3 are almost the same. The global minimum in this map is N2 at $\varphi$=80° and $\psi$=60°. All of three structures are characterized as GGGT. All of the low energy structures in the dielectric energy map do not form any intramolecular hydrogen bonds. This agrees with the deuterium exchange data. Since solvent-solute interactions are strong in the aqueous solution of GlcNAc( β 1,3)Gal( β ) OMe, intramolecular hydrogen bonds are weakened and replaced with solvent-solute hydrogen bonds. Therefore, the increased dielectric insulation effectively makes intramolecular hydrogen bonds weaker than those in vacuum and results in a feasible structure in solution. However, the low energy structure N2 and N3 do not reproduce the experimental structural constraints, it was neccesary to look at the dynamic behaviors of this carbohydrate.

In order to investigate the dynamic behavior of the GlcNAc( β 1,3)Gal( β )OMe on the adiabatic potential surface, molecular dynamics simulations on GlcNAc( β 1,3)Gal( β) OMe is proceeded. The low energy structures in the dielectric energy map are utilized for the initial structures of MD simulation. The dynamics trajectory is generated by following the standard dynamics procedure of the heating-equilibrium-production protocol as described in experimental section and entire trajectory of 100 psec is monitored with paying special attentions to confirmational transition.

The trajectory initiated from the N1 conformation is designated as the N 1 trajectory. The dihedral angles ($\varphi$, $\psi$, $\chi_1$, $\chi_2$, $\theta$), the interproton distances which corresponds to the short NOE contacts, and hydrogen bond distances obtained from each averaged vacuum dynameis trajectories are summarized in Table 5. As shown in Figure 8 the N1 trajectory generated in vacuum fluctuates around the N1 conformation. As shown in Figure 9, the intramolecular hydrogen bond, O 7'-OH3' and O2-NH' are maintained through the trajectory. Averaged O7'-OH3' distance is 1.9 Å and averaged O2-NH' distance is 2.3 Å during the trajectory. As shown in Figure 10a the exocyclic hydroxymethyl group of the GlcNAc moiety ($\chi_1$) does not make any transitions and is retained at GT orientation. However, that of galactose ($\chi_2$) undergoes transitions between GG and GT orientations as shown in Figure 10b. The orientation of N-acetyl group is maintained around 163° as listed in Table 5. The overall feature of the N1 conformation is retained.

The N2 trajectory shows transition pathway of N2-N1-N3-

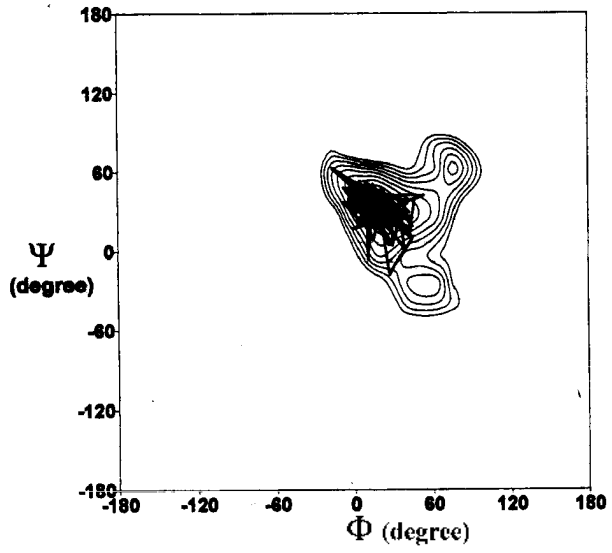


**Figure 8.** The N1 trajectory generated in vacuum on the ($\varphi$, $\psi$) plane, superimposed upon the vacuum energy map.

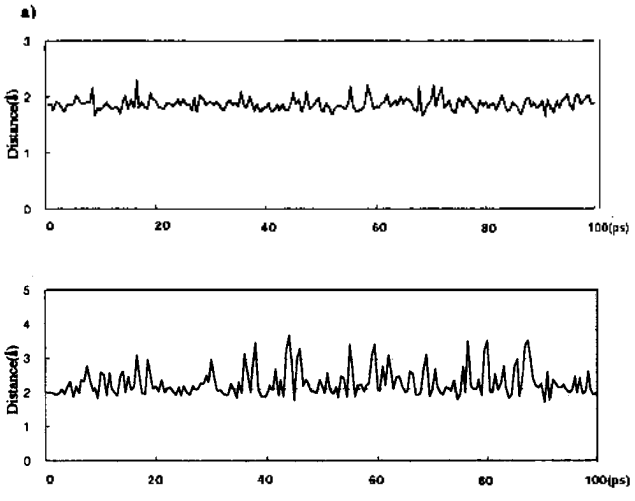


**Figure 9.** The intramolecular hydrogen bond distances during the N1 trajectory in vacuum, a) O7'-OH3' and b) O2-NH'.

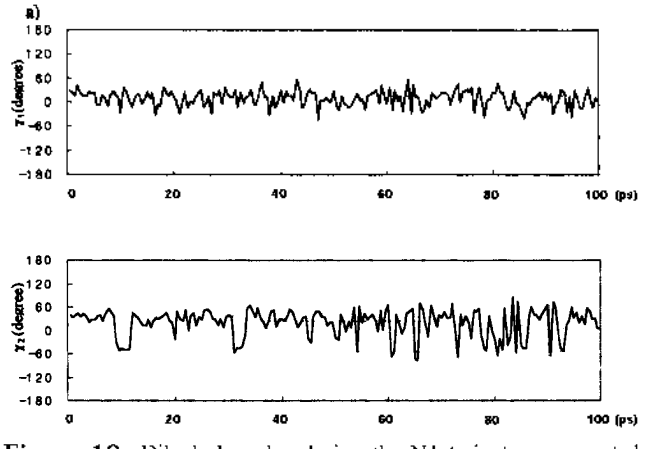


**Figure 10.** Dihedral angles during the N1 trajectory generated in vacuum, a) $\chi_1$(O5'-C5'-C6'-O6') b) $\chi_2$(O5-C5-C6-O6).

**Table 5.** Conformational features obtained from averaged dynamics trajectories generated in vacuum

| | N1 | N2 | N3 |
|---|---|---|---|
| $\varphi$ | 27.3(±12.7) | 36.5(±22.5) | 31.2(±17.4) |
| $\psi$ | 30.4(±11.7) | 30.9(±21.3) | 29.1(±18.2) |
| $\chi_1$ | 10.0(±20.0) | 8.7(±24.5) | 8.4(±23.2) |
| $\chi_2$ | 19.4(±36.0) | 11.0(±24.5) | 5.0(±23.0) |
| $\theta$ | 162.6(±12.2) | 166.9(±24.8) | 162.7(±14.6) |
| H1'-H2 | 3.5(±0.20) | 3.4(±0.40) | 3.5(±0.38) |
| H1'-H3 | 2.4(±0.15) | 2.5(±0.35) | 2.4(±0.24) |
| H1'-H4 | 4.3(±0.17) | 4.4(±0.32) | 4.3(±0.24) |
| O7'-OH3' | 1.9(±0.11) | 1.9(±0.13) | 1.9(±0.13) |
| O2-NH' | 2.3(±0.41) | 2.8(±0.98) | 2.6(±0.75) |

'numbers in the parenthesis are the rms deviations from the averaged values. Angles are in degree and distances are in Å.

N1 and ends up with the N1 conformation after 35 ps as shown in Figure 11. The intramolecular hydrogen bond, O7'-OH3' are maintained through the trajectory and the averaged O7'-O13' distance is 1.9 **Å**. However, the hydrogen bond, O2-O16' is broken at 10 ps and is not recovered and the averaged distance is 5.6 **Å** during the trajectory. The exocyclic orientation of the GlcNAc moiety ($\chi_1$) does not make transitions but that of galactose ($\chi_2$) undergoes transitions between GT and GG orientations. The orientation of N-acetyl group is maintained around 167°. The N3 trajectory shows transition pathway, N3-N1-N2-N1 and ends up with the N1 conformation after 85 ps as shown in Figure 12. The intramolecular hydrogen bond, O7'-OH3' are maintained through the trajectory and the averaged distances is 1.9 **Å**. The orientation of N-acetyl group is maintained around 163°, too. All of trajectories generated in vacuum ends up with N1 which is the lowest energy structure

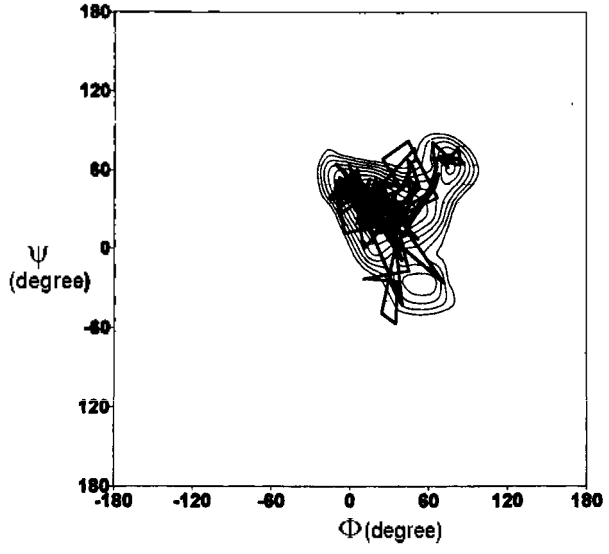


**Figure 11.** The N2 trajectory generated in vacuum on the (φ, ψ) plane, superimposed upon the N2 energy map.

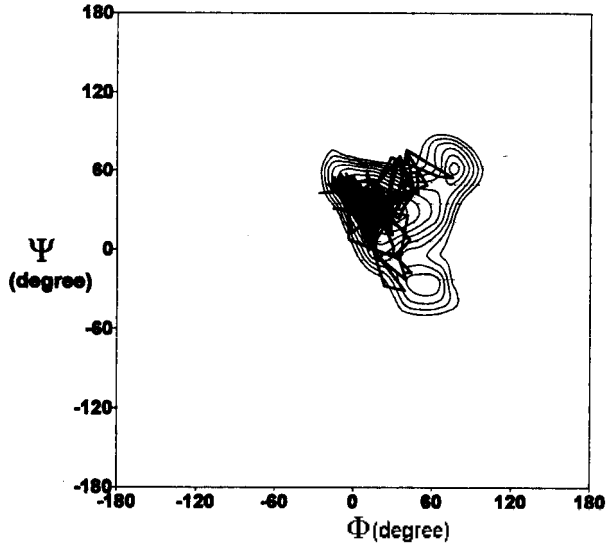


**Figure 12.** The N3 trajectory generated in vacuum on the (φ, ψ) plane, superimposed upon the N3 energy map.

in the vacuum map. Notice that even in N2 and N3 trajectories averaged distance of O2-NH' is shorter that 3.0 **Å** and weak hydrogen bond of O2-NH' is maintained in N2 and N3 trajectories.

In order to investigate the effects of the aqueous solvent effects on the dynamics of GlcNAc( β 1,3)Gal( β )OMe, the same set of dynamics simulations have been carried out with setting the dielectric constant to 50. Because increased dielectric shielding weakens intramolecular electrostatic interactions, there no longer appears the intramolecular hydrogen bonding pattern (C or R) around the ring. Figure 13 shows the N1 trajectory on the (φ, ψ) plane, superimposed upon the dielectric energy map. In contrast to the vacuum dynamics, the N1 trajectory generated with a dielectric constant of 50 shows the transition to the N3 conformation at the beginning and fluctuates between N2 and N3 regions. During the trajectory, the averaged distance of O7'-O13' and O2'-NH' are 4.3 **Å** and 4.9 **Å**, respectively. Therefore, there are no intramolecular hydrogen bonds in N1 trajectory generated with a dielectric constant of 50.

As the dielectric constant increases, the region near N2 becomes the global minimum in the dielectric energy map as shown in Table 4 and Figure 7. The N2 trajectory fluctuates mainly between the N2 and N3 conformations as shown in Figure 14. During the N2 trajectory the exocyclic orientation of the GlcNAc moiety ($\chi_1$) undergoes transitions between GG(-60°), GT(60°), and TG(180°) as shown in Figure 15a while the exocyclic orientation in vacuum trajectory is fixed at GT orientation. As described previously, coupling constant data proves that terminal exocyclic orientation of GlcNAc( β 1,3)Gal( β )OMe exists in a dynamic equilibrium of GG, GT, and TG orientations. N2 trajectory generated with a dielectric constant of 50 agrees well with the experimental coupling constant data. This terminal exocyclic orientation is very important in binding to the protein. When protein recognizes carbohydrates in the membrane, it prefers certain orientation of exocyclic hydroxymethyl group. Exocyclic orientation of the galactose moiety

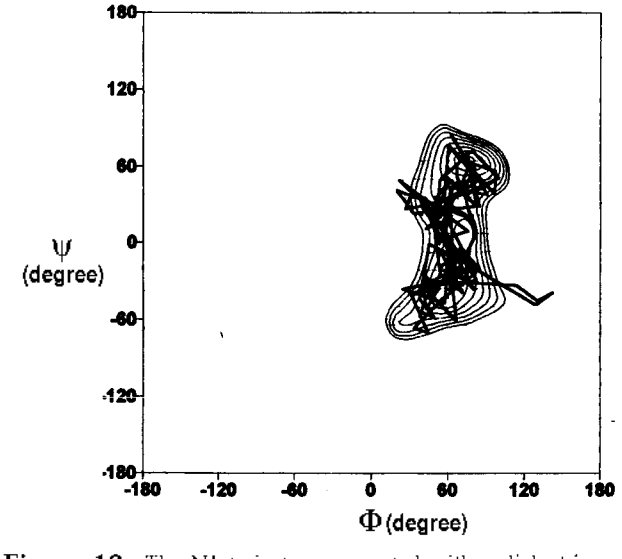


**Figure 13.** The N1 trajectory generated with a dielectric constant of 50 on the (φ, ψ) plane, superimposed upon the dielectic energy map.

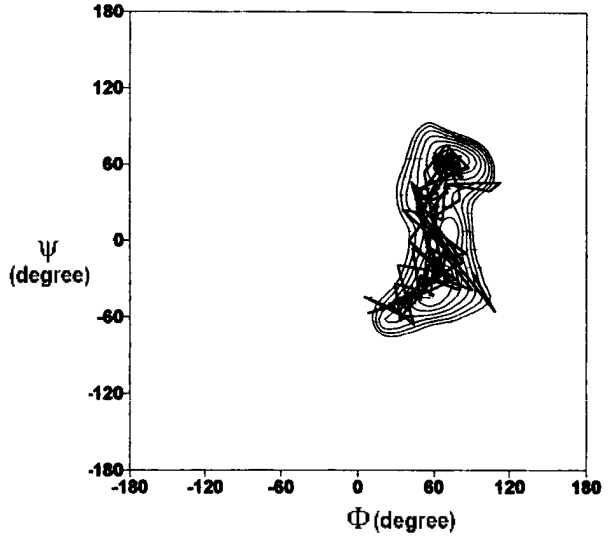


**Figure 14.** The N2 trajectory generated with a dielectric constant of 50 on the (φ, ψ) plane, superimposed upon the dielectic energy map.

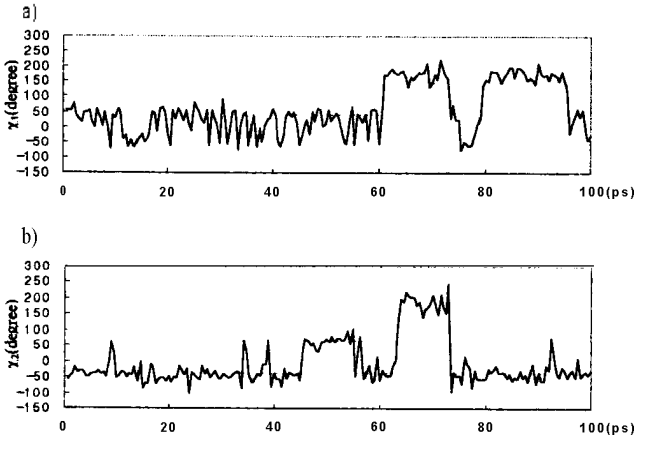


**Figure 15.** Exocyclic dihedral angles during the N2 trajectory generated with a dielectric constant of 50 a) $\chi_1$(O5'-C5'-C6'-O6'). b) $\chi$ (O5-C5-C6-O6).

($\chi_2$) also undergoes GG-GT-TG transitions as shown in Figure 15b. During the N2 trajectory the orientation of N-acetyl group is not maintained at certain orientation and fluctuates a lot as listed in Table 6. Dielectric insulation suppresses electrostatic interactions and thus results in more flexible molecular conformations. The N3 trajectory fluctuates between the N2 and N3 conformations as shown in Figure 16. During the N3 trajectory the exocyclic orientation of the GlcNAc moiety ($\chi_1$) undergoes GG-GT-TG transitions. Exocyclic orientation of the galactose moiety ($\chi_2$) also undergoes GG-GT-TG transitions, too. The dihedral angles (φ, ψ, $\chi_1$, $\chi_2$, θ) and the interproton distances which corresponds to the short NOE contacts obtained from each averaged dynamics trajectories are summarized in Table 6. All of trajectories generated with a dielectric constant of 50 fluctuates mainly between N2 and N3 regions, and they stay at the N3 region more than N2 region. GlcNAc( β 1,3)Gal( β )OMe exists in a dynamic equilibrium of N2 and N3 conformations and this is why N2 or N3 conformation by itself

**Table 6.** Conformational features obtained from averaged dynamics trajectories generated with a dielectric constant of 50

| | N1 | N2 | N3 |
|---|---|---|---|
| φ | 69.7(±31.2) | 63.8(±21.5) | 62.9(±15.7) |
| ψ | 3.9(±37.7) | 7.5(±44.7) | −12.3(±33.8) |
| $\chi_1$ | 42.3(±78.3) | 58.4(±82.1) | 42.7(±82.8) |
| $\chi_2$ | −24.7(±45.9) | −4.0(±75.6) | 13.9(±86.1) |
| θ | 83.1(±69.2) | 89.5(±68.0) | 79.2(±75.4) |
| H1'-H2 | 3.7(±0.63) | 3.6(±0.73) | 3.9(±0.60) |
| H1'-H3 | 2.7(±0.41) | 2.8(±0.42) | 2.6(±0.34) |
| H1'-H4 | 4.1(±0.56) | 4.0(±0.72) | 3.8(±0.52) |

[a] numbers in the parenthesis are the rms deviations from the averaged values. Angles are in degree and distances are in Å.

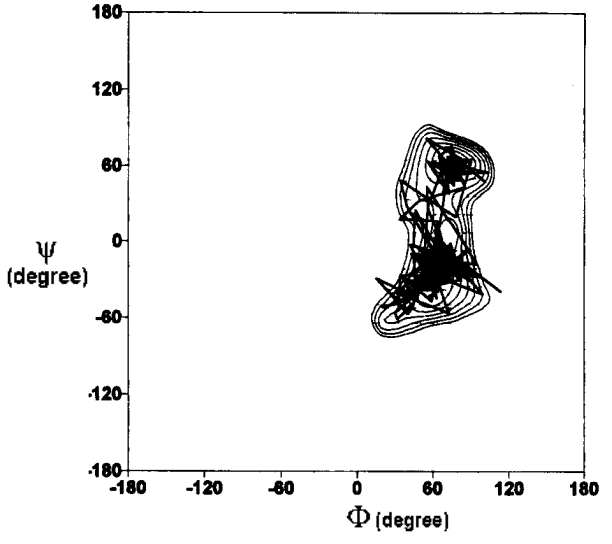


**Figure 16.** The N3 trajectory generated with a dielectric constant of 50 on the (φ, ψ) plane, superimposed upon the dielectic energy map.

can not reproduce the experimental NOE data.

The cross relaxation rate dominating the early portions of transfer between a pair of protons, after perturbing one proton, displays an inverse sixth power dependence on the interproton distance and provides very important structural informations. According to the previous NMR studies on lactose and melibiose, the rotational correlation time of these disaccharides are calculated as $10^{-11}$ sec.[8,9] Internal motions in carbohydrates can occur with a variety of time scales and with a variety of different amplitudes. If the internal motions are very fast compared to overall tumbling, experimental NOEs can be interpreted with a rigid model. However, if the internal motions become similar or slow compared to the overall tumbling time for a molecule and the motion is not isotropic, the situation becomes complicated. As long as the timescale of motion is short compared to the mixing time used for the NOE experiment, the effective relaxation rate for a pair of interacting spins will appear to be a simple average of the relaxation rate for each conformer. Because of the dynamic equilibrium existed in GlcNAc( β 1,3)Gal( β )OMe, fitting the NOE distance data to a single conformer would be unreasonable. If there is averaging between conformer 1 and 2, averaged relaxation

**Table 7.** RMSD values calculated by comparing experimental distances with the weighted average distances in two conformers

| Population ratio (N2 : N3) | RMSD |
|---|---|
| 100:0 | 0.60 |
| 80:20 | 0.31 |
| 60:40 | 0.19 |
| 40:60 | 0.16 |
| 20:80 | 0.23 |
| 0:100 | 0.61 |

rate between proton *i* and *j* can be expressed as follows.[13,14]

$$\sigma_{ij} = P_1 \cdot \sigma_{1ij} + P_2 \cdot \sigma_{2ij} \quad (3)$$

Here, $P_1$ and $P_2$ are the fractional populations of conformation 1 and 2, and $\sigma_{1ij}$ and $\sigma_{2ij}$ are the cross-relaxation rates between proton *i* and j for each conformer. Two state model was applied to the two low energy structures of N2 and N3 in the dielectric energy map. Table 7 shows the rms deviation values calculated by comparing the distances calculated from the experimental interring NOEs listed in Table 2 with the weighted average distances in two conformers. Weighted average distances are calculated from the cross relaxation rate of each conformers. N2 and N3 with various population ratio. Population ratio between N2 and N3 are changed from 100 : 0 to 0 : 100. If the ratio is 100 : 0, it is a single state model of N2 and it shows big deviations from the experimental NOEs. If the ratio is 0 : 100, it is a single state model of N3 and it also shows big deviations from the experimental NOEs. As shown in this table, two state model of N2 and N3 with a 40 : 60 population ratio fits the NOE well. From the adiabatic energy map, molecular dynamics simulation, and NMR experimental data we can conclude that there are flexibilities in the solution structrue of GlcNAc( β 1,3)Gal( β )OMe and it exists in a dynamic equilibrium between the two conformers, N2 and N3.

## Conclusion

In this study, the structure of carbohydrate, GlcNAc( β1,3) Gal( β )OMe was studied using nuclear magnetic resonance spectroscopy and molecular modeling. Diversity of the structure of this carbohydrate was studied as a recognition signal of protein. Adiabatic energy map offered detailed and useful information about the structure of GlcNAc( β 1,3)Gal( β )OMe. The lowest structure N1 in the adiabatic energy map generated in vacuum at φ=20° and ψ=40° reproduces the experimental structural constraints while N1 has intramolecular hydrogen bonds including O7'-OH3' and O2-NH'. Deuterium exchange experiment shows that amide proton in N-acetyl group does not form any intramolecular hydrogen bond. Therefore, in the vacuum energy map, the hydrogen bond is overemphasized and the structural features are different from the solution NMR experimental data.

Determination of solution structure of biomolecules using NMR data is commonly based on the assumption that the structure can be represented by a single rigid conformer. Since N1 which is the lowest energy structure in the vacuum map reproduces the experimental NOEs, single state model of N1 could be considered as the structure consistent with the experimental data. Global energy minimum structure N1 in vacuum map is different from the actual solution structure of GlcNAc( β 1,3)Gal( β )OMe is apparently due to an unphysical persistence of hydrogen bonds in vacuum which does not occur in aqueous solution. In order to represent the aqueous environment and flexible structures in solution, dielectric constant of 50 was used in generation of adiabatic energy map. In the adiabatic energy map generated with a dielectric constant of 50, N2 at φ=80° and ψ= 60° and N3 at φ=60° and ψ=−40° become the low energy structures. N1 trajectory generated with a dielectric constant of 50 shows transition to N2 and fluctuates mainly between N2 and N3 regions. Molecular dynamics simulations prove that GlcNAc( β 1,3)Gal( β )OMe exists in a motional averaging between N2 and N3 conformers. In order to represent this internal motion around the glycosidic bond, two state model was used to calculate the effective cross relaxation rate. Two state model of N2 and N3 conformers with a population ratio of 40 : 60 results in a good improvement in fit to cross-relaxation-derived distance constraints and represents the motional properties of GlcNAc( β 1,3)Gal( β )OMe very well. Data obtained from the solution NMR spectroscopy, adiabatic energy map, and molecular dynamics simulations on GlcNAc( β 1,3)Gal( β )OMe prove successfully that there are two distinct conformers of N2 and N3 in dynamics equilibrium.

From the $^3J_{5,6a}$, $^3J_{5,6b}$ coupling constant data and the molecular dynamics simulations the exocyclic orientation of the terminal GlcNAc ring is considered as an averaging of GG, GT, and TG orientations. The glycosidic dihedral angles, orientation of the N-acetyl group and the exocyclic orientation of GlcNAc( β 1,3)Gal( β )OMe can be a important factors of binding to the protein in the membrane. Even though GlcNAc( β 1,3)Gal( β )OMe can exist with a variety of motions, protein may exclude binding of a certain conformation on the basis of unfavorable interactions between the protein and the carbohydrate. Based on this structural details of GlcNAc( β 1,3)Gal( β )OMe interactions between this carbohydrate and the lectins will be studied.

**Acknowledgment.** This work was supported by the Basic Science Research Institute Program, Ministry of Education of Korea (BSRI-96-3442). Y. Kim thank National Institute of Safety Research of Korea for the partial support.

## References

1. Dwek, R. A. *Annu. Rev. Biochem.* **1993,** *62*, 65.
2. Sharon, N.; Lis, H. *Sci. Am.* **1993,** *268*, 74.
3. Lis, H.; Sharon, N. *Annu. Rev. Biochem.* **1986,** *55*, 35.
4. Etzler, M. E. *Annu. Rev. Plant. Physiol.* **1985,** *36*, 209.
5. Slomiany, B. L.; Banas-Gruszka, Z.; Zdebska, E.; Slomiany, A. *J. Biol. Chem.* **1982,** *257*, 9561.
6. Piller, F.; Cartron, J. P. *J. Biol. Chem.* **1984,** *259*, 13385.
7. John, F. K. *Carbohydrate chemistry;* Oxford University Press: New York, U. S. A., 1988; p 548.
8. Bevilacqua, V. C.; Thomson, D. S.; Prestegard, J. H. *Biochemistry* **1990,** *29*, 5529.
9. Bevilacqua, V. C.; Kim Y.; Prestegard, J. H. *Biochemistry* **1992,** *31*, 9339.
10. Cheong, Y.; Kang, D.; Kim, Y. submitted in Biochem-

istry.
11. Oh, J.; Kim, Y.; Won, Y. *Bulletin Korean Chem. Soc.* **1995,** *16,* 1153.
12. Ha, S. N.; Madsen, L. J.; Brady, J. W. *Biopolymers* **1988,** *27,* 1927.
13. Kim, Y.; Ohlrogge, J. B.; Prestegard, J. *Biochemical Pharmacology* **1990,** *40,* 7.
14. Kim, Y.; Prestegard, J. *Biochemistry* **1989,** *28,* 8792
15. Molecular Simulation Inc., San Diego, CA.
16. Bax, A.; Subramanial, S. *J. Magn. Reson.* **1986,** *67,* 565.
17. Ichikawa, Y.; Lin, Y.; Dumas, D. P.; Shen, G. J.; Garcia-Junceda, E.; Williams, M. A.; Bayer, R.; Ketcham, C.; Walker, L. E.; Paulson, J. C.; Wong, C. *J. Am. Chem. Soc.* **1992,** *114,* 9283.
18. Neuhaus A.; keeler, J. *J. Magn. Reson.* **1986,** *68,* 568.
19. Bothner-By, A. A.; Stephens, R. L.; Lee, J. M.; Warren, C. D.; Jeanloz, R. W. *J. Am. Chem. Soc.* **1984,** *106,* 811.
20. Haasnoot, C. A. G.; De Leeuw, F. A. A. M.; Altona, C. *Tetrahedron* **1980,** *36,* 2783.
21. Brooks, S. R.; Bruccoleir, R. E.; Olafson, B. D.; States, D. J.; Swaminathan, S.; Karplus, M. *J. Comput. Chem.* **1983,** *4,* 187.

# Hyperfine Interaction Integrals for NMR Chemical Shifts in 5f Paramagnetic Systems

**Kee Hag Lee*, Ji Young Lee, and Dong Hee Kim**

*Department of Chemistry, WonKwang University, Iksan 570-749, Korea*
*[†]Department of Chemistry, Kunsan National University, Kunsan 573-701, Korea*

*Received February 10, 1997*

To study the NMR chemical shift arising from the 5f-electron orbital angular momentum and the 5f-electron spin dipolar-nuclear spin angular momentum interactions, the evaluation of the hyperfine integrals has been extended to any pairs of SCF type 5f orbitals adopting a general method which is applicable to a general vector ***R,*** pointing in any direction in space. From the electronic wavefunctions for 5f orbitals expressed in common coordinate system, the radial part of the hyperfine interaction integrals are derived by translating the exponential part, $r^{-1}\exp(-2\beta r)$, in terms of $\boldsymbol{R}$, $\boldsymbol{r}_1$ and the modified Bessel functions. The radial integals for 5f orbitals are tabulated in analytical forms. When two of the hyperfine integrals along the (100), (010), (001), (110), and (111) axes are calculated using the derived radial integrals, the calculated values for the 5f system change sign for R-values larger than R≃0.35 nm. But the calculated values for the 4f systems change sign for R-values larger than R≃0.20 nm.

## Introduction

In the past two decades a substantial amount of work has been devoted toward evaluation of the contact and pseudo contact contributions to the observed isotropic shifts in the $^1$H nuclear magnetic resonance (NMR) spectra of uranium (IV) organometallic compounds.[1-5] Nuclei in different molecular electronic environments experience different shielding field and such differences in shielding field give rise to the chemical shifts in high resolution NMR spectroscopy. The chemical shifts are extremely important in the applications of NMR to molecular structure studies. The interpretation of the NMR shift in 5f paramagnetic systems has been based on the Fermi contact interactions and pseudo contact interactions. A large number of organometallic actinide compounds have been synthesized and their NMR spectra in solution are studied. Much of this NMR work has been reviewed by Fischer[6] and by Luke and Streitwieser.[7] In those cases in which the pseudo contact shift could be reliably estimated, it was found that when the pseudo contact shift was subtracted from the experimental shift a sizeable shift, which has generally been called the contact shift, remained. The results of the pseudo contact interaction were interpreted using the dipolar approximation expressed in terms of the magnetic susceptibility components.[8] But Golding *et al.*,[9-11,14] Ahn *et al.*[12,13] and Lee and Lee *et al.*[15] have shown that the use of such an expression may lead to serious errors in the interpretation of the NMR shift through this mechanism, especially if only the dipolar term is considered.

Since our interest is centered on the NMR shift arising from the 5f-electron orbital angular momentum and the 5f-electron spin dipolar-nuclear spin angular momentum interactions for an 5f-electron in a crystal field environment centered at $O_{xyzXYZ}$, it is necessary to evaluate the theoretical hamiltonian representing the pseudo contact part,[16]

$$H_{\parallel} = H + H_{\perp} \tag{1}$$

where

$$\boldsymbol{H}_{\perp} = \frac{2\mu_0}{4\pi} g_N \mu_B \mu_N \{\boldsymbol{I}_N \cdot \boldsymbol{I}/r_N^3\} \tag{2a}$$